TURBULENT SHALLOW FLOW THROUGH VEGETATION

GUILLERMO PALAU SALVADOR

Rural Engineering Department, Polytechnic University of Valencia, 46022, Valencia, Spain

THORSTEN STOESSER

School of Civil and Environmental Eng., Georgia Inst. of Tech., Atlanta, 30332, GA, USA

ANDREAS CHRISTOF RUMMEL

Department of Civil and Environmental Engineering, University of Genoa, 16145 Genoa, Italy

WOLFGANG RODI

Institute for Hydromechanics, University of Karlsruhe, 76128 Karlsruhe, Germany

Abstract. A solid understanding of the flow through plant canopies is important to better understand river and coastal restoration schemes or the creation of flood retention activities. Large Eddy Simulations (LES) were performed for open channel flow through emergent vegetation at shallow flow conditions. The vegetation is idealized with rigid cylinders of constant diameter d. The results are compared to surface velocities measured with help of a 2D Particle Image Velocimetry (PIV) system. The main objective of this paper is to gain insight into the mean and instantaneous flow fields, turbulence and momentum exchange as well as the complex interaction between the flow and the vegetation elements. The Reynolds number based on the channel depth h and the bulk velocity u_b is approximately $Re_h \approx 3{,}000$. Due to flow separation at the cylinder, vortices are shed and the formation of a von Karman type vortex street is visible. However, one of the major novelties in this flow type is that the vortices are strongly influenced by the neighboring cylinders located in streamwise and spanwise directions and experimental and numerical investigations are rare. A good match between computed and experimental quantities, both turbulences intensities and mean values, was found.

1. INTRODUCTION AND BACKGROUND

Both aquatic and riparian vegetation have become central to river and coastal restoration schemes, the creation of flood retention space and coastal protection projects. Aquatic and riparian plants obstruct the flow and reduce the mean flow velocities relative to non-vegetated regions, and the additional pressure and viscous drag exerted by plants influences strongly the mean and instantaneous

flow field as well as transport processes and system morphology. A greater understanding of the interaction of flow with vegetation is needed in order to improve our ability to accurately model flow and sediment transport through vegetation.

Most research activities on vegetation effects in the riparian environment have been devoted to laboratory flumes of simple cross-section, and many researchers e.g. [1,2,3] have made progress in understanding the mean flow In the surface flow layer above a submerged vegetation zone, researchers (e.g. [1]) have generally assumed that the logarithmic law prevails. However, detailed laboratory studies of flow-vegetation interaction and the consequences on the instantaneous flow field, bed-shear stresses, drag and friction relationships and the consequences for transport processes are rare.

Presently, steady Reynolds Averaged Navier Stokes (RANS) models are the most practical approaches for high-Reynolds-number-fluvial hydraulics applications despite the rapid advancements in computational power and numerical algorithm development. These steady RANS models allow the resolution of the time-averaged turbulent flow field by adding a subgrid force to the RANS and turbulence transport equations to account for vegetative drag effects. For multi-dimensional flow problems, such methods were used by [4,5,6,t] together with a k-ε or k-ω turbulence closure models to study the mean flow through submerged vegetation. [8 and 9] used a Reynold's Stress model (RSM) accounting for the anisotropy of turbulence, to simulate the flow through rigid submerged vegetation elements. However, although mean velocities were predicted with satisfying accuracy, RANS models have been less successful at correctly predicting streamwise and vertical turbulence intensities, because these models cannot account for organized large-scale unsteadiness and asymmetries (coherent structures) resulting from turbulent flow instabilities.

Recently, Large Eddy Simulations (LES) of such flows that directly resolve large-scale, organized, unsteady structures in the flow were presented [10 and 11]. LES is able to elucidate the large-scale coherent structures described above, their important role in vegetative resistance, and the interaction and feedback between the region within and outside the vegetation layer.

In this paper we present Large-Eddy simulations of turbulent channel flow through a matrix of cylinders. The flow around the individual cylinders is fully resolved by a high resolution grid and the cylinder-matrix can be regarded as an idealized vegetation layer. The time-averaged velocity field as well as turbulence quantities are presented and compared with laboratory measurements.

2. COMPUTATIONAL AND EXPERIMENTAL FRAMEWORK AND SETUP

The simulations were performed with the code HYDRO3D-GT, a successor of the code HYDRO3D originally developed at Bristol, University [12]. The code solves the filtered Navier-Stokes equations on curvilinear grids. Second-order central differences are employed for the convective as well as for the diffusive terms. A fractional-step method is used with a Runge-Kutta predictor and the solution of a pressure-correction equation in the final step as a corrector. The original Smagorinsky model [13] is used to approximate the subgrid-scale stresses that appear from the filtering procedure. The no-slip wall boundary condition is used at the vegetation stems and at the bottom wall and the free surface is set as a rigid lid with a slip condition. Periodic boundary conditions are applied in the streamwise and spanwise directions assuming geometrical and statistical homogeneity of the flow.

Setup and boundary conditions were selected in analogy to laboratory experiments carried out to provide validation data for the simulations. Surface velocities were measured with a 2D PTV system. It consists of a double-camera setup with 10 Hz frame rate and continuous floodlight was used as illumination. Floating 2mm round-shaped black polypropylene particles on a white background were used as seeding. A PTV-algorithm was then applied to derive velocity vectors for each single particle and afterwards a standard bi-cubic interpolation algorithm was used to redistribute velocities on a regular grid for a better comparison with results from simulations.

The Re number, based on the channel depth h and bulk velocity u_{bulk} is approximately *3000*. The computational domain spans *20D* in streamwise, *10D* in spanwise and h (which is the full water depth) in vertical direction, respectively. The grid consisted of a total of approximately 7 Million grid points. The grid spacings in terms of wall units in stream- and spanwise directions were $\Delta x^+ = \Delta y^+ \approx$ 50-60 in the region between the cylinders and $\Delta x^+ = \Delta y^+ \approx 1$ near the cylinder surface. In the vertical the grid was stretched towards the free surface and values of $\Delta z^+ \approx 60$ near the water surface and $\Delta z^+ \approx 1$ near the near the channel bed were obtained.

3. RESULTS AND DISCUSSION

3.1. *Mean Flow Statistics*

Figure 1 presents contours of the mean streamwise (left) and spanwise (right) velocities at the free surface. For comparison the measured values are overlaid as

black contour lines. The vegetal elements obstruct the flow and reduced velocities can be seen in an area behind the cylinders. Maximum streamwise and spanwise velocities are found where the flow accelerates around the cylinders. Overall the agreement is fairly good; the obvious mismatch near the vegetal elements can be attributed to the sparse particle density in the recirculation region close to the circular cylinder.

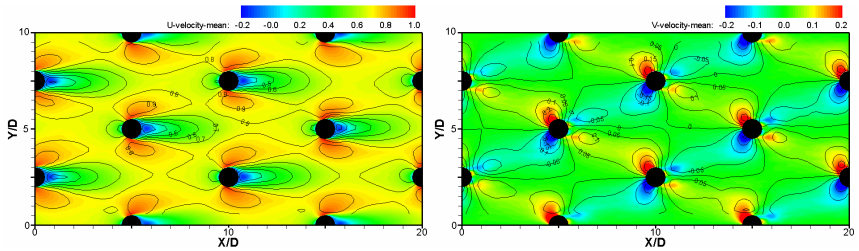

Figure 1. Distribution of mean streamwise (left) and spanwise (right) surface velocities.

Figure 2 presents contours of streamwise (left) and spanwise (right) turbulent fluctuations at the free surface. High streamwise turbulent fluctuations can be seen on either side of the cylinder where the flow separates from the cylinder. The peak of the spanwise fluctuations is found just behind the average recirculation region. Again, the overall agreement is fairly good; Near the cylinders the fluctuations are underestimated by the PIV system due to the lack of resolution.

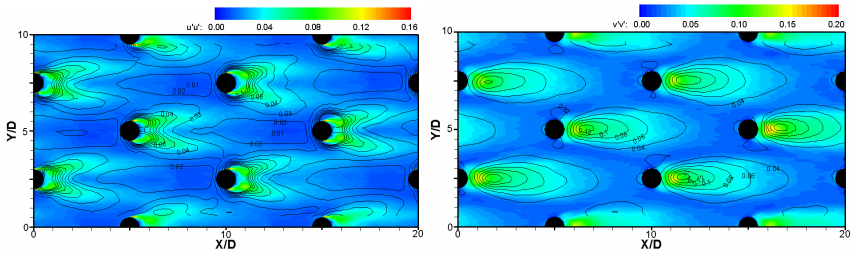

Figure 2. Distribution of streamwise (left) and spanwise (right) turbulent fluctuations at the free surface.

3.2. *Instantaneous Flow*

The distribution of the instantaneous streamwise velocity is presented in Figure 3. Immediately apparent is the formation of a low-momentum wake behind the elements which is a result from the formation of von-Karman type vortex streets. Also apparent is the in-phase shedding of the elements aligned perpendicular to the flow.

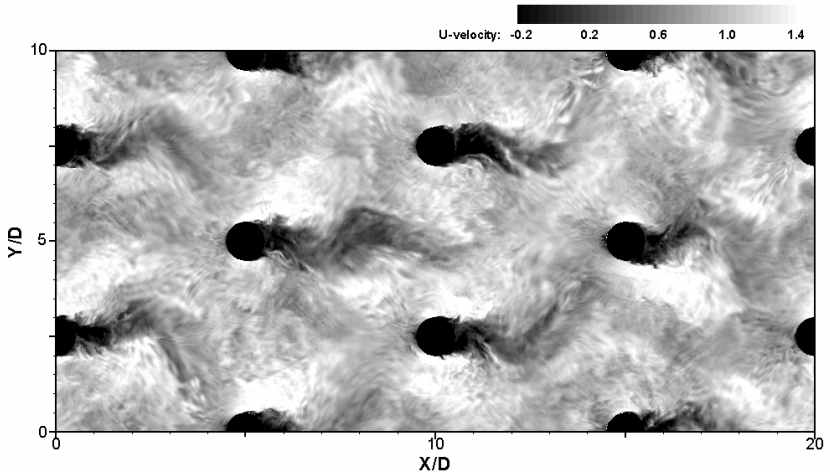

Figure 3. Distribution of instantaneous streamwise surface velocities.

3.3. *Bed Shear Stress Distribution*

Figure 4 shows the distribution of the mean (left) and instantaneous (right) bed-shear stress made dimensionless with the total shear stress $\tau(mean) = \sqrt{\rho g h} = dp/dx\,h$. Maximum values which are in the order of 20% of the total shear-stress are found close to the cylinders where the flow accelerates around the stems. Negative values can be detected in the recirculation region and in front of the cylinders, where downwards directed fluid along the cylinder surface generates a fairly strong reverse flow. Instantaneous bed-shear stresses have maxima in the order of 25% of the total shear stress. Larger patches of high shear-stress are found near the elements as well as in the shear layer of the wake and are a result of the formation of the horseshoe vortex wrapping around the vegetal elements as well as von-Karman type vortices that are shed from the elements.

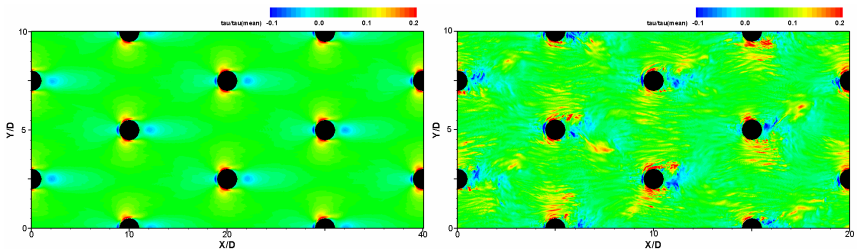

Figure 4. Distribution of mean (left) and instantaneous (right) bed-shear stresses normalized with the total shear-stress.

4. CONCLUSIONS

Large eddy simulations were performed for turbulent flow through emergent vegetation. Additional PIV measurements of surface velocities were carried out to provide validation data for the simulations. Overall fairly good agreement was obtained for the distribution of surface flow quantities. Instantaneous flow structures such as von-Karman type vortices and horseshoe vortex formation are responsible for bed-shear stress peaks, however most of the energy losses are shown to be due to the drag exerted by the plants.

5. ACKNOWLEDGEMENTS

A.C.R. was supported by an E.U. EST-020228 FLUBIO grant during his stay in Genova.

References

1. Kouwen N., Unny T.E., Hill H.M. *ASCE J. of Irrigation and Drainage Division, 95: 329-342.* (1969).
2. Dunn, C., Lopez F., Garcia, M. H.. *Hydraul. Engr. Series No. 51, UILU-ENG-96-2009*, UIUC. (1996).
3. Nepf, H.M. and Vivoni, E.R. *ASCE Wetlands Engineering and River Restoration Conference. Denver, CO*. (1998).
4. Shimizu, Y. and Tsujimoto, T. *J. of Hydroscience and Hydraulic Engrg., JSCE, Vol. 11, No. 2, pp. 57-67*. (1994).
5. Lopez, F. and Garcia M. *ASCE J. Hydraulic Engrg., 127(5), 392-402*. (2001).
6. Fischer Antze, T., Stoesser, T., Bates, P. B. and Olsen, N. R. *IAHR Journal of Hydraulic Research 39: 303 - 310*. (2001).
7. Neary, V. S. ASCE Journal of Eng. Mechanics. 129(5), 558-563. (2003).
8. Naot, D., Nezu, I. and Nakagawa, H. ASCE J. Hydraulic Engrg., 122 (11): 625 – 633. (1996).
9. Choi S. U. and Kang H. Proc. XXIX IAHR Congress, Beijing, China. (2001).
10. Cui, J. and Neary V.S. Proc. Hydroinformatics, Cardiff, UK. (2002).
11. Stoesser, T., Liang, C. and Rodi, W. Proc. Riverflow, Lisbon, Portugal. (2006).
12. Stoesser, T. PhD. Thesis, Dep. Civil Eng., Bristol University. (2002).
13. Smagorinsky, W. Monthly Weather Review. (1963).